J. Fluid Mech. (2000), *vol.* 420, *pp.* 259–276. Printed in the United Kingdom

Miscible rectilinear displacements with gravity override. Part 2. Heterogeneous porous media

By EMMANUEL CAMHI, ECKART MEIBURG† AND MICHAEL RUITH

Department of Aerospace and Mechanical Engineering, University of Southern California, Los Angeles, CA 90089-1191, USA

(Received 7 January 2000 and in revised form 16 May 2000)

The effects of permeability heterogeneities on rectilinear displacements with viscosity contrast and density variations are investigated computationally by means of direct numerical simulations. Physical interpretations are given in terms of mutual interactions among the three vorticity components related to viscous, density and permeability effects. In homogeneous environments the combined effect of the unfavourable viscosity gradient and the potential velocity field generated by the horizontal boundaries was seen to produce a focusing mechanism that resulted in the formation of a strong vorticity layer and the related growth of a dominant gravity tongue (Ruith & Meiburg 2000). The more randomly distributed vorticity associated with the heterogeneities tends to 'defocus' this interaction, thereby preventing the formation of the vorticity layer and the gravity tongue. When compared to neutrally buoyant flows, the level of heterogeneity affects the breakthrough recovery quite differently. For moderate heterogeneities, a gravity tongue still forms and leads to early breakthrough, whereas the same result is accomplished for large heterogeneities by channelling. At intermediate levels of heterogeneity, these tendencies partially cancel each other, so that the breakthrough recovery reaches a maximum. Similarly, the dependence of the breakthrough recovery on the correlation length is quite different in displacements with density contrasts compared to neutrally buoyant flows. For neutrally buoyant flows the resonant interaction between viscosity and permeability vorticities typically leads to a minimal recovery at intermediate values of the correlation length. In contrast, displacements with density contrast give rise to a gravity tongue for both very small and very large values of this length, so that the recovery reaches a maximum at intermediate values.

1. Introduction

The companion paper by Ruith & Meiburg (2000) (part 1) investigated displacements of fluids of variable viscosity and density in a homogeneous porous medium. Particular attention was paid to the dynamic interactions among the two associated vorticity modes and the potential flow generated by the impermeable boundaries at the top and bottom of the reservoir. This potential velocity component was found to result in a 'focusing' effect, which locally amplifies the viscous fingering instability by causing an increased flow rate near the top of the reservoir. This mechanism, which

† To whom correspondence should be addressed, present address: Department of Mechanical and Environmental Engineering, University of California, Santa Barbara, CA 93110, USA, e-mail: meiburg@engineering.ucsb.edu

is responsible for the emergence of a narrow gravity tongue, was seen to dominate the displacement in certain parameter regimes. It is then natural to ask how these dynamic interactions will be modulated by the existence of heterogeneities in the porous medium. This topic is addressed by the present investigation.

The understanding of constant density and viscosity flows in heterogeneous porous media, the so-called tracer flow problem, has reached an advanced stage, see the reviews by Dagan (1987); Koch & Brady (1988), as well as the discussion and references provided by Tchelepi (1994). In the presence of viscosity and/or density differences, the dynamics of displacement processes in heterogeneous media become significantly more complex, due to the introduction of additional length and time scales into the problem. Depending on the relative magnitude of these scales, the interaction among the various physical mechanisms can be more or less pronounced. Tan & Homsy (1992) as well as DeWit & Homsy (1997*a*, *b*) provide an interesting example of this behaviour in their computational investigation of neutrally buoyant, variable-viscosity rectilinear displacements in heterogeneous porous media. They show that a resonant interaction between viscosity- and permeability-driven effects can occur when these act on comparable length scales, with the result of minimal recovery efficiency. The existence of this resonance phenomenon was confirmed by Chen & Meiburg (1998*b*) for the quarter five-spot geometry, which is not an obvious result since the length scale of the fingering instability increases continuously as the front spreads from the injection well to larger radii.

The simulations by Tchelepi (1994) also address the problem of rectilinear flows in heterogeneous media. This author performs extensive parameter variations in order to outline the boundaries between 'heterogeneity-dominated' and 'fingering-dominated' displacements. The dependence of the recovery curves on the viscosity ratio as well as on the properties of the heterogeneity field is documented, even past the breakthrough point. His main findings are that the recovery decreases as the mobility ratio becomes more unfavourable, and as the level of heterogeneity increases. Tchelepi does observe a certain dependence on the transverse correlation length, but he does not comment on the 'resonance phenomenon' described earlier by Tan & Homsy (1992). It seems possible that this might be due to the properties of his numerical approach, which does not resolve the detailed effects of physical diffusion/dispersion at the front. As a result, the optimal coupling between the preferred wavelength of the viscous fingering instability and the corresponding intermediate correlation length may not have been captured. Further computational investigations that addressed viscous fingering in the presence of permeability heterogeneities were conducted by Waggoner, Castillo & Lake (1992), Sorbie *et al.* (1992), and Araktingi & Orr (1993). All of these authors employ velocity–pressure formulations of the governing equations.

Tchelepi (1994) also conducts a number of large-scale simulations to investigate the interplay of viscous, density, and permeability effects. He points out that the balances among the associated forces can shift with time and location, and that the early stages are usually dominated by the forces related to viscous and permeability effects. While he does not systematically investigate the dependence of these interactions on the correlation length and the level of the heterogeneities, he finds that the particular random realization of the heterogeneity field can have a large influence on the properties of the ensuing displacement. Specifically, he observes that for different heterogeneity fields characterized by identical global quantities, the recovery may or may not depend monotonically on the ratio of viscous to gravitational forces. Both Tchelepi (1994) as well as Moisses, Miller & Wheeler (1989) in their investigation of the role of permeability heterogeneities base their simulations on the more conventional

pressure–velocity formulation of the governing equations. As has been pointed out by several authors, this form of the equations has the disadvantage of not allowing a clear distinction between the effects of viscosity and density contrasts, and permeability heterogeneities. In this regard, the alternative streamfunction–vorticity formulation offers certain advantages. The goal of the present investigation is then to fully resolve the diffusive concentration profile at the front, and to analyse the mutual interactions among viscosity-, permeability-, and density-driven effects in terms of their vorticity dynamics, as a function of the fluid properties and the features of the heterogeneity field.

2. Governing equations

In the presence of a spatially varying normalized permeability field $k = k(\boldsymbol{x})$, the dimensionless governing equations derived in part 1 take the form

$$\nabla \cdot \boldsymbol{u} = 0, \tag{2.1a}$$

$$\nabla p = -\frac{\mu}{k}\boldsymbol{u} - G\rho\nabla y, \tag{2.1b}$$

$$\frac{\partial c}{\partial t} + \boldsymbol{u} \cdot \nabla c = \frac{1}{Pe}\nabla^2 c, \tag{2.1c}$$

$$\mu(c) = \mathrm{e}^{R(1-c)}. \tag{2.1d}$$

The governing dimensionless parameters are Pe, G, R, and A, as defined and described in part 1. In addition, the spatial distribution of the normalized heterogeneous permeability field enters into the problem. It is characterized by correlation lengths in the x- and y-directions, as well as by a variance, as will be explained below.

By proceeding analogously to part 1 and recasting the continuity equation and Darcy's law into the vorticity (ω) and streamfunction (ψ) formulation, we obtain

$$\nabla^2 \psi = -\omega, \tag{2.2a}$$

$$\omega = -R\nabla\psi \cdot \nabla c - \frac{1}{k}\nabla\psi \cdot \nabla k + \frac{Gk}{\mu}c_x. \tag{2.2b}$$

It is interesting to note that the vorticity equation (2.2*b*) now contains three components that can interact with each other: in addition to the viscosity- and gravity-related vorticity fields discussed in part 1, there now appears a contribution related to the variations in the permeability field (Tan & Homsy 1992). In the following, we will refer to these components as viscosity, gravity, and permeability vorticity, respectively. The interaction between permeability and viscosity vorticity was analysed in detail by Chen & Meiburg (1998*b*) for the plane quarter five-spot geometry, i.e. in the absence of density differences. To our knowledge the coupling between gravity and permeability vorticities, and the ways in which gravity vorticity modulates the interaction between permeability and viscosity components, has not yet been investigated. A first interesting observation from the above equations is that the local permeability appears in the numerator of the gravity vorticity. This indicates that, in contrast to the homogeneous case analysed in part 1, the integral over the gravity vorticity, i.e. the gravity circulation

$$\Gamma_G = \int_S \omega_G \, \mathrm{d}S, \qquad \omega_G = \frac{Gk}{\mu}c_x \tag{2.3}$$

is no longer constant in time, and instead can vary as the concentration front reaches

regions of different local permeability values. This raises the possibility for the gravity vorticity to interact with the other vorticity components in a fundamentally different way, compared to homogeneous flows. It is particularly noteworthy that the gravity vorticity term contains the combination k/μ, i.e. the mobility. Since fluid of low viscosity will preferentially move into regions of high permeability, the gravity vorticity may reach locally large values as the concentration front moves through areas of high permeability. This suggests that the predominantly one-way coupling between gravitational and viscous vorticity components (as discussed in part 1) may be more two-way in nature in the presence of permeability heterogeneities. The study of this interaction will be a main focus of the present investigation.

Boundary and initial conditions for the numerical simulations are set correspondingly to part 1. The numerical solution technique is identical to part 1 as well, i.e. it employs a Fourier series approach in the streamwise direction (Gottlieb & Orszag 1977), sixth-order compact finite differences (Lele 1992) in the vertical direction, and an explicit third-order Runge–Kutta time-stepping scheme (Wray 1991).

2.1. *Permeability field*

In order to generate the desired statistical distribution of the permeability field, we use an algorithm provided by Shinozuka & Jen (1972). This algorithm was employed successfully by Tan & Homsy (1992) for rectinilear flows without density differences, as well as by Meiburg & Chen (1998*b*) for the quarter five-spot geometry. It yields the permeability field $k(\boldsymbol{x})$ as the exponential of a random function $f(\boldsymbol{x})$, whose Gaussian distribution is characterized by the variance s and the covariance R_{ff}. The latter in turn depends on the spatial correlation scales l_x in the longitudinal, and l_y in the transverse direction. With $\langle , \rangle$ indicating the autocovariance, we thus have

$$k(\boldsymbol{x}) = \mathrm{e}^{f(\boldsymbol{x})}, \tag{2.4a}$$

$$\langle f, f \rangle = s^2 R_{ff}(\boldsymbol{x}), \tag{2.4b}$$

$$R_{ff} = \exp\left(-\pi\left[\left(\frac{x}{l_x}\right)^2 + \left(\frac{y}{l_y}\right)^2\right]\right). \tag{2.4c}$$

Of course, this model is not be applicable to all porous media, as the heterogeneities in some materials may obey different statistical laws. In order to be able to apply the same numerical approach as in part 1 of the present investigation, we demand $k_z = 0$ at the inflow and outflow boundaries. This choice is justified by the observations made in part 1, as well as by Tchelepi (1994), that the outflow boundary affects the nature of the flow only over a very short distance in the upstream direction. At the upper and lower boundaries of the domain, we specify $k_y = 0$, which allows us to extend the high-order numerical discretization all the way to these boundaries. These boundary conditions of vanishing normal derivative are implemented in the same way as described in Chen & Meiburg (1998*b*). In the present investigation, we employ permeability heterogeneity fields with correlation lengths ranging from 0.02 to 0.2, and variances up to $s = 0.8$. These parameter values generate ratios of maximum to minimum permeability of up to $O(100)$.

3. Results

As was done in part 1 for homogeneous diplacements, the basic features and mechanisms dominating heterogeneous miscible displacements will first be illustrated and

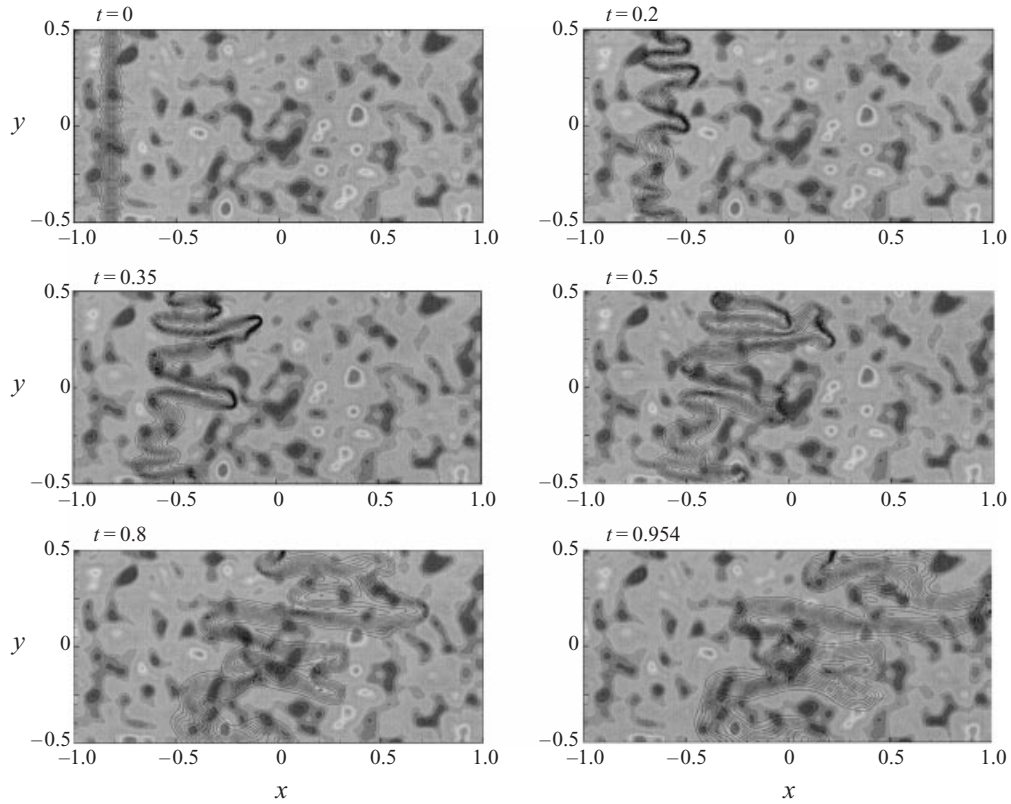

FIGURE 1. Reference case: $Pe = 500$, $G = 1$, $R = 2$, $A = 0.5$, $s = 0.5$, and $l = 0.1$. The concentration field is shown at times $t = 0$, 0.2, 0.35, 0.5, 0.8, 0.954. The heterogeneity leads to the early appearance of several fingers. While overall the displacement proceeds faster in the upper half of the domain, the narrow, dominant gravity tongue of the homogeneous flow (cf. figure 2) does not emerge.

discussed by means of a reference case. In this way, the role of the permeability heterogeneities, and the way in which they modulate the interaction between the gravity and viscosity vorticity components, will be clarified. Subsequently, the dependence of the flow on some of the dimensionless parameters will be addressed. In the course of performing test simulations, it was found that for constant Pe-values, the presence of heterogeneities led to steeper concentration fronts. As a result, we had to lower the Péclet number for our reference case to 500, instead of the 2000 employed in part 1.

3.1. *Reference case*

Figure 1 displays the evolution of the displacement for $Pe = 500$, $G = 1$, $R = 2$, $A = 0.5$, $s = 0.5$, and $l_x = l_y = l = 0.1$. The corresponding homogeneous case with an identical initial concentration field is depicted in figure 2. A comparison of these figures demonstrates that, for the present parameters, the heterogeneity promotes the early appearance of several fingers. While these are predominantly found in the upper half of the domain, there is a sizable finger developing near the bottom boundary as well. By comparing the evolving frontal shape with the features of the permeability field, we recognize that for the present level of heterogeneity the injected fluid has a strong tendency to follow paths of high permeability. In addition, the tip splitting

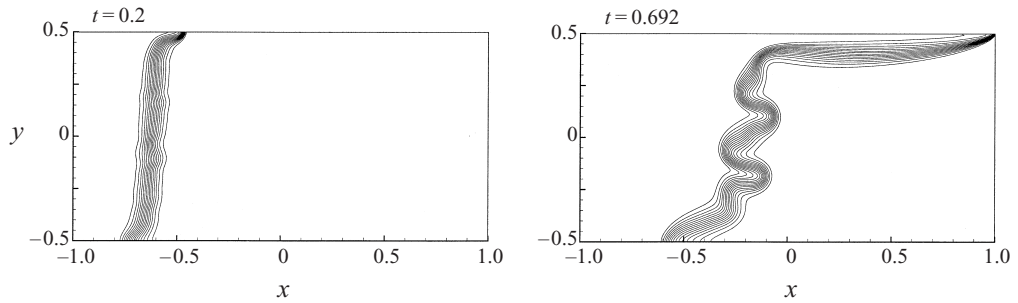

FIGURE 2. The homogeneous flow for $Pe = 500$, $G = 1$, $R = 2$, and $A = 0.5$, at times $t = 0.2$ and 0.692. In the absence of heterogeneities, fingering evolves much more slowly, and the flow is quickly dominated by a narrow gravity tongue that propagates along the upper boundary of the domain.

event observed around $t = 0.5$ is triggered by the local features of the permeability field as well.

Interestingly, in the heterogeneous displacement the influence of the gravitational effects does not manifest itself in the form of a gravity tongue propagating along the upper boundary of the reservoir, as it does in the homogeneous case. While overall the fingers in the upper half of the domain are observed to grow and propagate more rapidly than those near the lower border, the most advanced finger is located approximately one third of the domain height below the upper boundary.

In part 1, the importance of the potential flow field was pointed out, which forms through the combined effects of the gravitational vorticity and the horizontal borders of the domain. It was demonstrated that the interaction of the viscous vorticity with this potential flow field leads to a focusing effect, which results in the narrow, dominant gravity tongue propagating along the top of the domain. From the comparison of the displacements in figures 1 and 2 it thus appears that the heterogeneities prevent this sharp focusing, and instead distribute the effects of gravitational override over a wider region. An important consequence is that the heterogeneous displacement breaks through considerably *later* than in the corresponding homogeneous flow, in spite of generating pronounced fingers after a much shorter time. Comparisons by Chen & Meiburg (1998*a*, *b*) of neutrally buoyant quarter five-spot displacements had shown the heterogeneous case to always break through *earlier* than the homogeneous flow. This represents a first indication that the role of heterogeneities in miscible displacements with density override is fundamentally different from neutrally buoyant flows. The reasons for these differences can be found in the mutual interations of the various vorticity components.

Figures 3–6 depict the overall vorticity field, as well as the three individual vorticity components, of the reference flow at times 0.2 and 0.8. The location of the front is indicated by the iso-concentration contours 0.05 and 0.95. While both the gravity and viscosity vorticities are limited to the frontal region, their distributions show distinctly different features. The viscosity vorticity tends to form predominantly horizontal layers that are aligned with the evolving fingers, i.e. in regions with strong y-components of the concentration gradient. The gravitational vorticity, on the other hand, is associated with the x-component of the concentration gradient, i.e. with the vertical sections of the concentration front. In contrast to the above two vorticity components, the permeability vorticity is distributed throughout the entire domain in a somewhat random fashion, with larger amplitudes appearing in areas of higher velocity magnitudes. Initially, the features of this random distribution are dominated

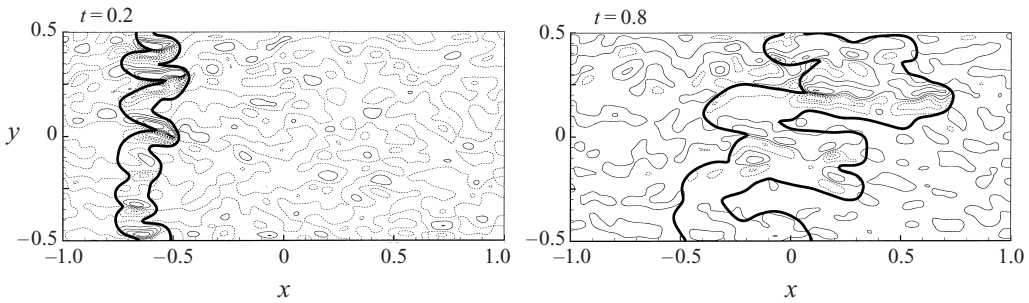

FIGURE 3. Isocontours of the overall vorticity of the flow in figure 1 at times $t = 0.2$ and 0.8. The location of the concentration front is indicated by the 0.05 and 0.95 concentration contours. Within the front, the structures of the vorticity field display a higher level of coherence, while they are more randomly distributed throughout the rest of the domain.

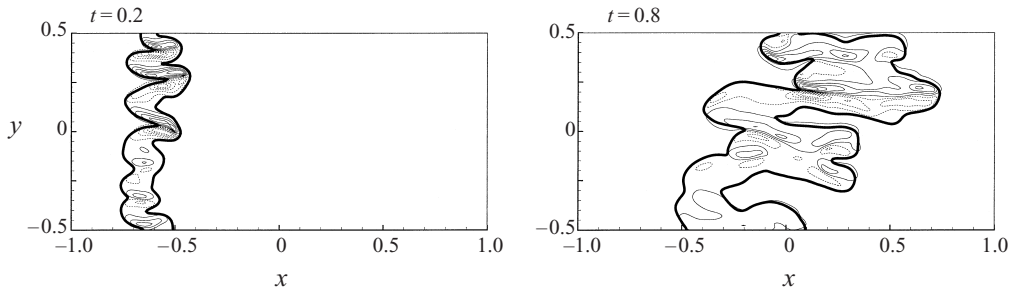

FIGURE 4. Isocontours of the viscosity vorticity of the flow in figure 1 at times $t = 0.2$ and 0.8. This vorticity component tends to form layered dipole structures within the evolving fingers.

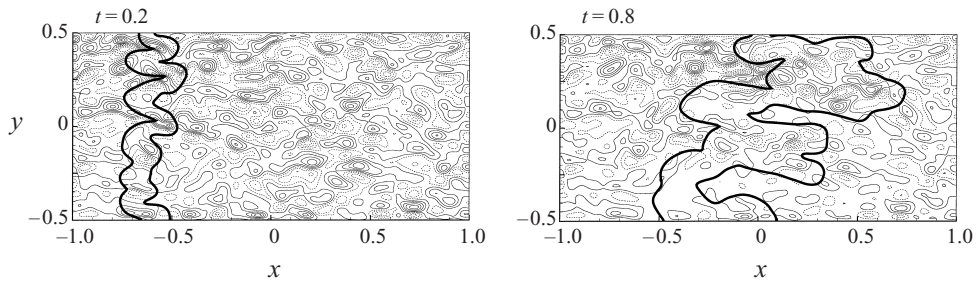

FIGURE 5. Isocontours of the permeability vorticity of the flow in figure 1 at times $t = 0.2$ and 0.8. Within the front, this vorticity component strongly interacts with the viscosity vorticity component. In the process, the two amplify each other (cf. Chen & Meiburg 1998*b*), which is reflected by the permeability viscosity. Outside the front, the permeability vorticity is distributed more randomly. The locally higher amplitudes in the upper part of the domain indicate an overall larger displacement velocity in this region.

by the interaction of the still nearly uniform flow with the permeability field, so that they reflect the variance and correlation length of the latter. As the displacement evolves, significant velocity components are induced by the gravitational and viscosity effects, with higher velocity values appearing near the upper border of the domain and inside the fingers. Consequently, the permeability vorticity assumes larger values in these regions as well. However, it still shows strong fluctuations at a length scale

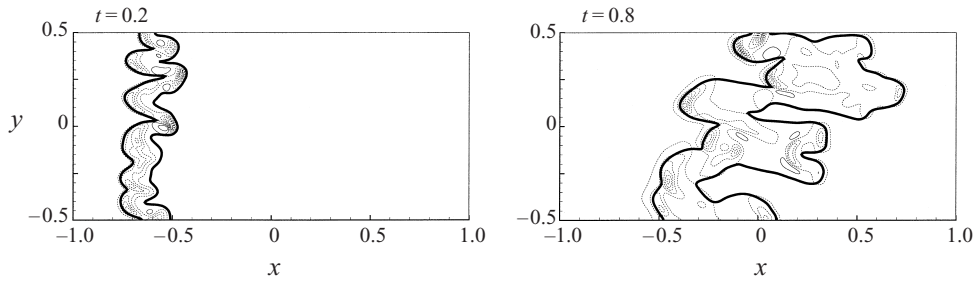

FIGURE 6. Isocontours of the gravity vorticity of the flow in figure 1 at times $t = 0.2$ and 0.8. This vorticity component is predominantly of one sign, and it is preferentially located in regions with large horizontal concentration gradients, i.e. along vertical sections of the front.

reflecting the permeability heterogeneities. These fluctuations will then also be found in the velocity field associated with the permeability heterogeneities.

It is instructive to track the evolution of the individual circulation components as a function of time. In analogy to the gravity circulation Γ_G, we define the viscous and permeability circulations, respectively, as

$$\Gamma_v = \int_S -R\nabla\psi \cdot \nabla c \, \mathrm{d}S, \qquad \Gamma_P = \int_S -\frac{1}{k}\nabla\psi \cdot \nabla k \, \mathrm{d}S. \tag{3.1}$$

Figure 7(*a*) shows how these circulation components, as well as their sum, develop as a function of time. For comparison, figure 7(*b*) shows the corresponding homogeneous case. We notice that for the present combination of the governing parameters, the gravity circulation does not vary much from its homogeneous value. This indicates that, at least in an integral sense, the gravity circulation plays similar roles in the homogeneous and heterogeneous displacements. More surprising is the persistently positive value of the permeability circulation component. In a neutrally buoyant displacement, one would expect this component to be zero on average. The positive value of Γ_P indicates that the permeability circulation is counteracting the effect of the gravity circulation, i.e. on average it reduces the tendency of the fluid to propagate more rapidly along the top of the reservoir, and more slowly along the bottom.

In order to eliminate the possibility that this behaviour is an artifact of the particular random realization of the permeability field, we carried out an additional simulation for an identical set of parameters, but a 'flipped' permeability field. This flipped permeability distribution was obtained by exchanging the original heterogeneity values at y and $-y$. In neutrally buoyant displacements, the permeability circulation of the flipped case should be of equal magnitude and opposite sign to the original case. However, we found that in the flipped case it hovered around zero, cf. figure 7(*c*). We hence conclude that there is a systematic trend for the permeability vorticity to counteract the effects of the gravity vorticity. In order to understand the detailed reasons for this behaviour, it is best to focus on the dominant term in the permeability vorticity, i.e. $-uk_y/k$. Consider a typical high-permeability channel with a permeability distribution as sketched in figure 7(*d*). In a neutrally buoyant flow, the displacing, less-viscous fluid will flow along the centre of the channel, and it will be symmetrically distributed around the channel centreline. However, if the displacing fluid is lighter than the displaced phase, it will on average rise slightly above the centreline. As a result, the effective viscosity above the channel centreline will be somewhat lower than below the centreline. This, in turn, leads to slightly larger u-velocities above the

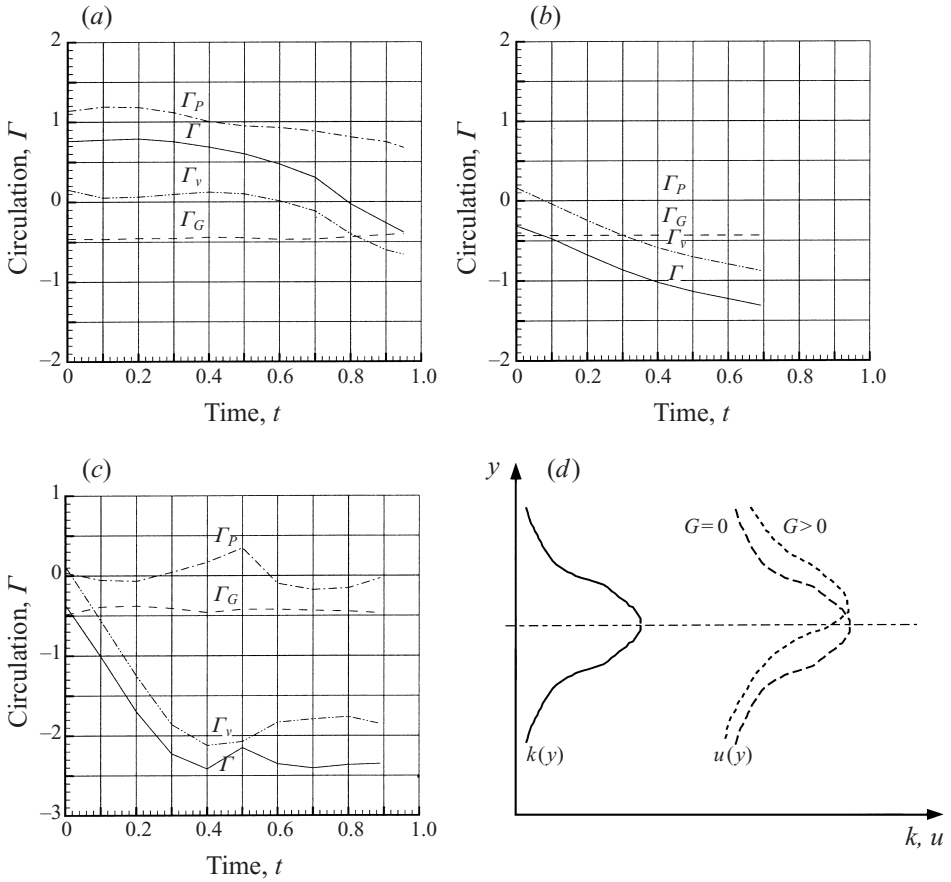

FIGURE 7. Viscosity, permeability, gravity and overall circulation as a function of time for (*a*) the reference case, (*b*) the corresponding homogeneous case, (*c*) the reference case, but with a flipped permeability field. The tendency of the permeability circulation to assume positive values is explained in the text, based on the permeability and velocity profiles sketched in (*d*).

channel centreline than below. Overall, this behaviour has the effect that in the regions above (below) the channel centreline, where $k_y < 0$ ($k_y > 0$), the magnitude of the permeability vorticity increases (decreases). Thus the positive (negative) permeability vorticity values are amplified (damped), so that the permeability circulation on average is shifted towards positive values. This tendency of the permeabilty vorticity to counteract the effects of the gravity vorticity is primarily responsible for the delay in breakthrough caused by the heterogeneities.

3.2. *Role of the permeability heterogeneities*

In the following, we will analyse the mutual interaction mechanisms among the different vorticity components and the potential velocity component generated by the conditions at the top and bottom boundaries, as a function of the governing dimensionless parameters.

3.2.1. *Basic considerations*

In order to understand how even moderate permeability heterogeneities are able to prevent the formation of the gravity tongue, it is interesting to analyse the way in

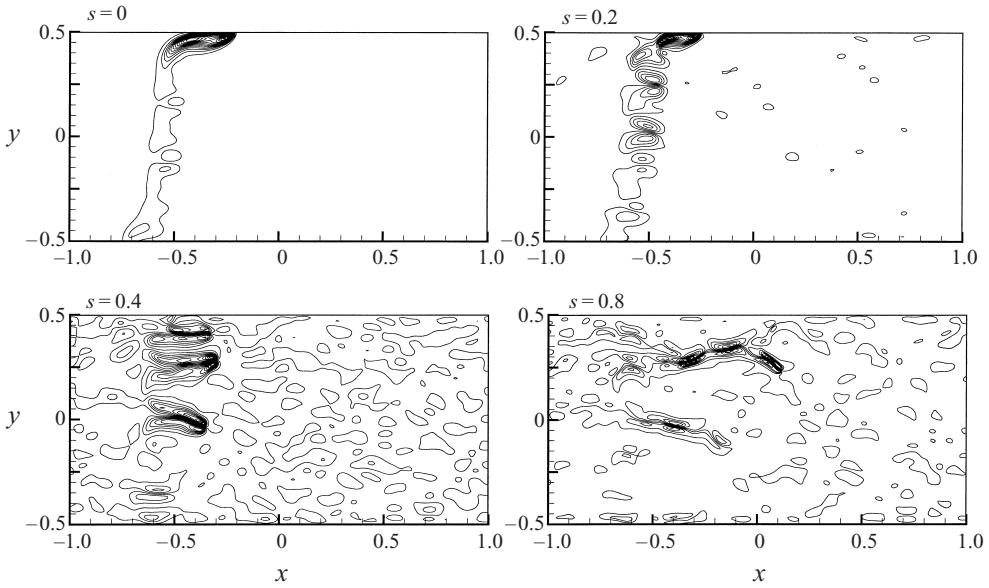

FIGURE 8. Vorticity at time $t = 0.3$ for $Pe = 500$, $G = 1$, $R = 2$, $A = 0.5$, $l = 0.1$, as well as $s = 0$, 0.2, 0.4, and 0.8. Increasing levels of heterogeneity are seen to break up the evolving vorticity layer at the underside of the gravity tongue, thereby defocusing the interaction between the viscosity vorticity on one hand, and the gravity vorticity in combination with the related potential velocity field on the other.

which the permeability vorticity affects the interaction between the viscosity vorticity and the gravity vorticity, as well as the related potential velocity field. The random fluctuations in the vorticity and velocity field due to the heterogeneity prevent the formation of the strong, uninterrupted vorticity layer along the upper section of the front that was found to be associated with the focusing effect in part 1. Instead, the emerging vorticity layer is broken up by the permeability heterogeneities. This breakup is clearly demonstrated by figure 8, which depicts the overall vorticity field at identical times for different levels of heterogeneity. At the same time, the mutual interaction of permeability and viscosity vorticity encourages a fingering process that is more uniformly distributed along the entire front. Taken together, these mechanisms result in the 'defocusing' of the interaction between the viscous vorticity on one hand and the gravitational vorticity in combination with the related potential velocity field on the other.

3.2.2. *Influence of the variance*

Figure 9 displays the concentration front at the time of breakthrough for the same parameter values as in the reference case, except that $s = 0$, 0.2, 0.4, and 0.8, respectively. For $s = 0.2$, we still notice a strong similarity of the front to the homogeneous case. Obviously, this low level of heterogeneity does not prevent the formation of a pronounced, narrow gravity tongue propagating along the upper border of the domain, as a result of the focusing mechanism described in part 1. At the same time, the fingers below the gravity tongue have evolved farther than in the homogeneous case, apparently encouraged in their growth by the mild heterogeneities. This mutual amplification of the viscosity and permeability vorticity components, as previously explained by Chen & Meiburg (1998*b*), leads to a more uniform fingering

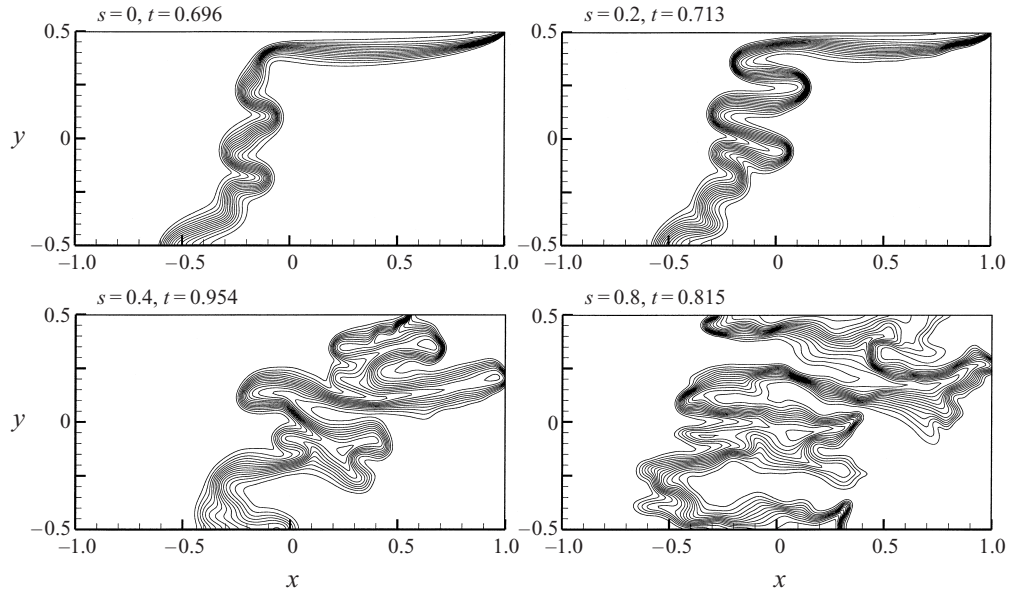

FIGURE 9. Concentration front at the time of breakthrough for $Pe = 500$, $G = 1$, $R = 2$, $A = 0.5$, $l = 0.1$, and $s = 0$, 0.2, 0.4, and 0.8, respectively. Intermediate values of the heterogeneity variance s lead to the latest breakthrough times, i.e., to the highest recovery rates.

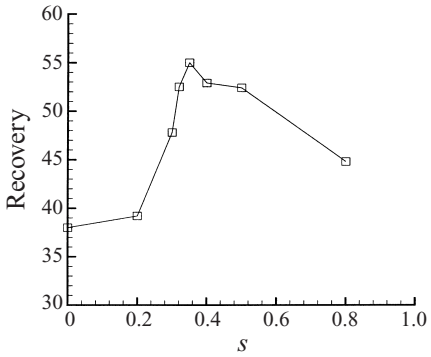

FIGURE 10. Breakthrough recovery as a function of the heterogeneity level s for $Pe = 500$, $G = 1$, $R = 2$, $A = 0.5$, and $l = 0.1$. Optimal recovery is obtained for intermediate values. For lower values of s, the tendency to form a gravity tongue leads to an early breakthrough, while for higher values the same outcome is achieved by the emergence of a dominant, narrow channel of less-viscous fluid.

across the front, and thereby to a slowdown of the gravity tongue, and consequently a delay of the breakthrough, compared to the homogeneous case. As s is further increased to 0.4, this feedback loop between viscosity and permeability vorticity gains in strength, and it dominates over the focusing mechanism, so that a pronounced gravity tongue no longer emerges. At the even larger values of $s = 0.5$ (the reference case, cf. figure 1) and 0.8, the mutual amplification between these two vorticity components is sufficiently strong for one or two fingers to quickly dominate the entire flow field, suppress the growth of other fingers, and lead to an early breakthrough.

The above series of simulations shows that, as far as the breakthrough recovery is concerned, there exists an optimal heterogeneity level at which the tendency to form a

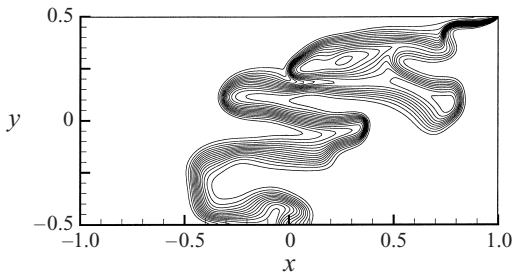

FIGURE 11. Concentration front at the time of breakthrough for $Pe = 500$, $G = 1$, $R = 2$, $A = 0.5$, $s = 0.5$, and $l = 0.2$. For $l = 0.1$, these parameter values had not shown a gravity tongue. The fact that a gravity tongue appears for $l = 0.2$ indicates that the mutual amplification of viscosity and permeability vorticity is not as pronounced for the larger correlation length. As a result, the tendency towards forming a gravity tongue wins over that towards forming narrow, low viscosity flow channels in the interior of the domain.

gravity tongue (as a result of the interaction of the viscous vorticity component with the gravitational component and the associated potential velocity field) is just balanced by the tendency to form narrow channels of the less-viscous fluid (due to the mutual amplification of the viscous and permeability vorticity components). Deviations from this optimal s-value result in one of these mechanisms dominating over the other one, with the outcome of a reduced breakthrough time. The breakthrough recovery as a function of s shown in figure 10 hence has a clear maximum for intermediate values. This finding is in complete contrast to our earlier observations for neutrally buoyant displacements, where the breakthrough recovery declined monotonically with increasing values of the variance. In this context, it is necessary to recall that part 1 had shown the aspect ratio A to be an important parameter in determining whether or not a gravity tongue will emerge. Specifically, longer domains with larger flow times were more likely to lead to the formation of a gravity tongue. As a result, it is to be expected that the optimal s-value will depend on the aspect ratio as well. A quantitative analysis of this dependence has not been performed within the present investigation.

3.2.3. *Influence of the correlation length*

Previous investigations of heterogeneous, neutrally buoyant, rectilinear (Tan & Homsy 1992) and quarter five-spot flows (Chen & Meiburg 1998*b*) demonstrated that the viscosity and permeability vorticities interact most strongly when the associated length scales are comparable. This optimal coupling between the viscosity and permeability vorticity components was termed a resonance phenomenon by Tan & Homsy. Consequently, since the optimal value of s is determined by the balance between the tendency to form a gravity tongue on one hand, and the coupled effects of permeability and viscosity vorticity on the other, we expect the heterogeneity variance associated with the highest breakthrough recovery to vary as a function of the correlation length l. This is confirmed by figure 11, which shows a displacement for the same parameter values as the reference case, except that $l = 0.2$. We observe the emergence of a gravity tongue even at this comparatively large s-value, for which the channelling tendency had dominated the $l = 0.1$ case. The flow is characterized by fewer and wider structures as a result of the increased correlation length. At the opposite end of the spectrum, i.e. for values of l that are considerably smaller than the diffusive length scale of the front, we expect to observe the formation of a gravity tongue as well, since such a medium appears homogeneous to the flow (Chen & Meiburg 1998*b*).

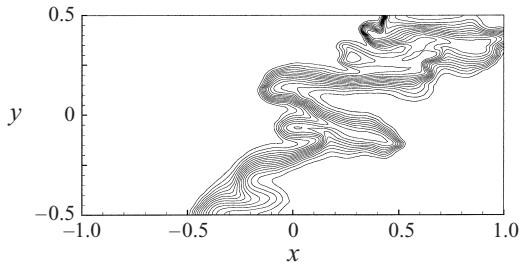

FIGURE 12. Concentration front at the time of breakthrough for $Pe = 500$, $G = 1$, $R = 2$, $A = 0.5$, $s = 0.5$, and $l = 0.02$. Even for this small correlation length, a gravity tongue does not form, as there is still a substantial interaction between the permeability and viscosity vorticity components.

From the above, it thus is obvious that the dependence of the breakthrough recovery on the correlation length in two-dimensional rectilinear displacements with density differences is diametrically opposed to that observed in neutrally buoyant flows (Tan & Homsy 1992; Chen & Meiburg 1998*b*). For the latter, intermediate correlation lengths resulted in the earliest breakthrough, as a consequence of the above mentioned resonance mechanism. In the presence of density differences, however, a gravity tongue will form both for very small and very large values of l, thereby resulting in an early breakthrough. Only for intermediate l-values can the interaction between viscous and permeability vorticity be sufficiently strong to suppress the formation of this tongue, so that breakthrough will be delayed.

Figure 12 shows that a correlation length of $l = 0.02$ apparently is not yet in the asymptotic range where the medium appears to be homogeneous to the displacement, since a clear gravity tongue does not yet form. The reason for this behaviour is that even at this small correlation length, there still is a substantial level of interaction between the viscosity and permeability vorticities. This may be somewhat surprising, considering the much larger 'natural' length scale of the viscous fingers observed for these parameters in the homogeneous case (figure 2). However, it is to be kept in mind that the specific numerical values at which all of the above findings are made may vary somewhat with the particular random realization of the heterogeneity distribution. In other words, one particular distribution may favour the formation of a gravity tongue, while another one may discourage it. This point will be addressed in some more detail below. For this reason, all of the simulations for $l = 0.1$ had used identical heterogeneity distributions (with varying amplitudes), so that the above observations would not be obscured by the variations in the random distributions.

3.2.4. *Different random realizations*

In order to evaluate the effects of differences between individual random realizations of the heterogeneity distribution, we carried out several pairs of simulations in which all parameters including the initial concentration distribution were held constant. The only difference is that one simulation employs the 'original' heterogeneity distribution, while the other one uses the 'flipped' distribution, described above. Figure 13 depicts such a pair of simulations for the parameter values $Pe = 500$, $G = 2$, $R = 2$, $A = 0.5$, $s = 0.8$, and $l = 0.1$. Substantial differences between the two displacements are visible. In particular, in one flow the breakthrough is caused by a gravity tongue, while in the other one it is not. The breakthrough recovery is more than one-third higher in the latter case. Obviously, for this relatively high s-value, the differences between different

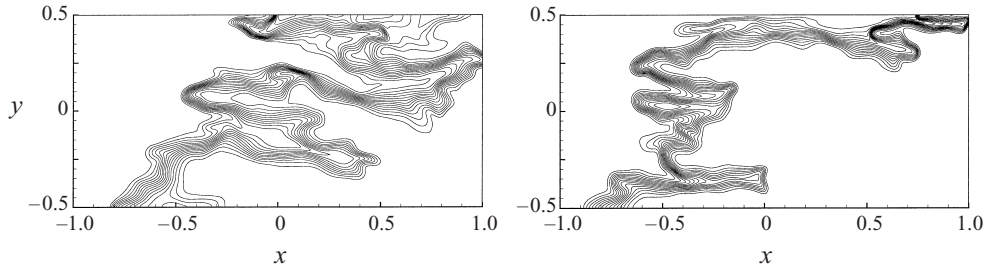

FIGURE 13. $Pe = 500$, $G = 2$, $R = 2$, $A = 0.5$, $s = 0.8$, and $l = 0.1$: comparison at breakthrough of the respective displacements for the 'original' and 'flipped' heterogeneity distributions. For these large levels of heterogeneity, substantial differences can be obtained for different heterogeneity distributions characterized by the same global values of l and s.

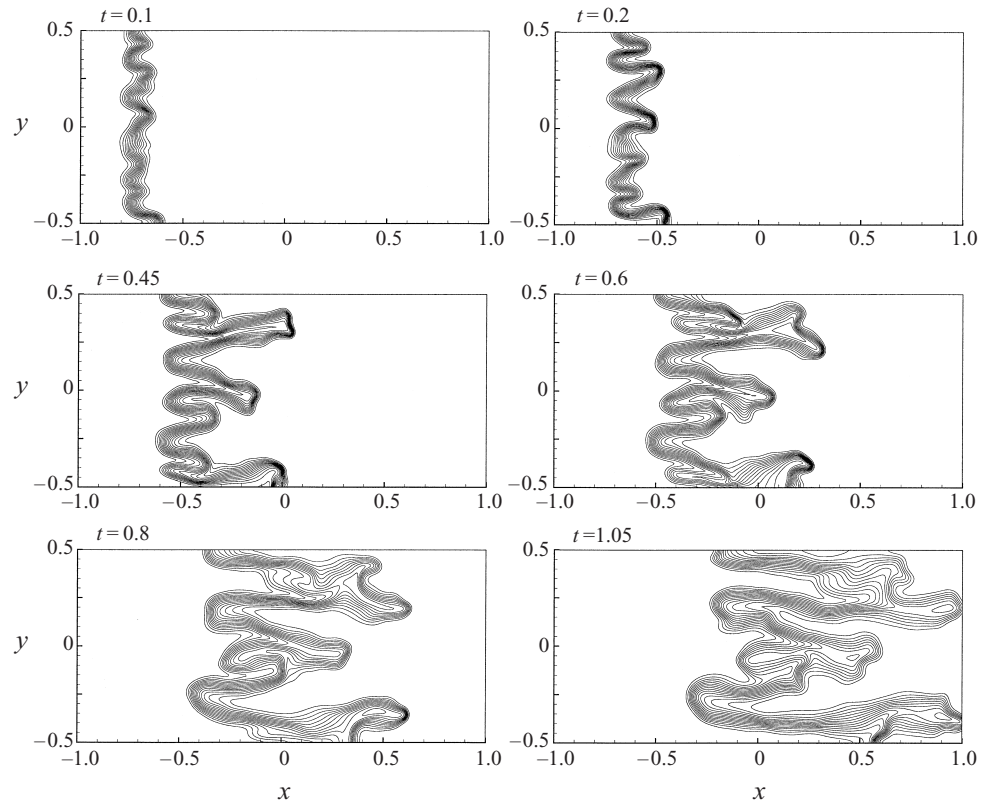

FIGURE 14. Concentration field for $Pe = 500$, $G = 0$, $R = 2$, $A = 0.5$, $s = 0.5$, and $l = 0.1$ at times $t = 0.1$, 0.2, 0.45, 0.6, 0.8, and 1.05. In the absence of density differences, the displacement proceeds at roughly equal rates in the upper and lower sections of the domain.

random realizations are quite pronounced. These differences are expected to be much milder for lower levels of heterogeneity.

3.3. *Influence of gravity parameter G*

In order to elucidate the influence of the gravity parameter, we conducted a simulation for the same parameters as in the reference case, except that $G = 0$, see figure 14. Initially, the concentration front develops quite similarly to the reference case. However, the fingers near the top grow somewhat more slowly, and the ones near

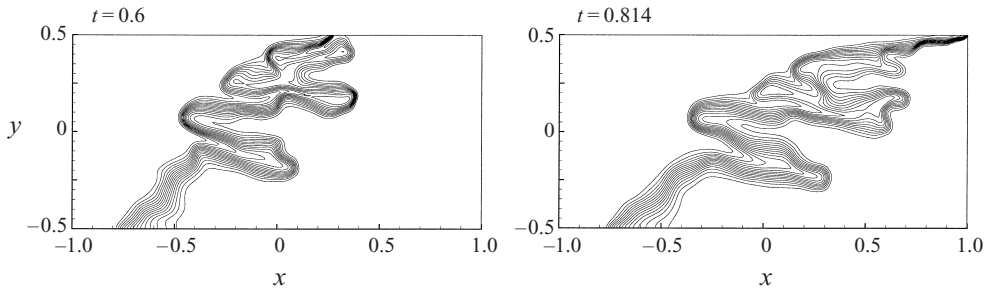

FIGURE 15. Concentration field for $Pe = 500$, $G = 2$, $R = 2$, $A = 0.5$, $s = 0.5$, and $l = 0.1$ at times $t = 0.6$ and 0.814. At this higher density contrast, a gravity tongue evolves even in a strongly heterogeneous medium.

the bottom slightly faster, suggesting that in the reference case gravity led to an effective override by redirecting displacing fluid into the upper half of the domain. This observation is further confirmed by the case $G = 2$ shown in figure 15. Here the fingering develops even more rapidly in the upper half of the domain. In addition, during the late stages a dominant gravity tongue emerges along the upper boundary. This indicates that a certain level of heterogeneity is able to prevent the formation of a narrow gravity tongue only for G-values up to a certain level. If gravitational effects are sufficiently strong, a dominant gravity tongue will form even in an environment characterized by more pronounced heterogeneities. Consequently, the above findings regarding the optimal s-value are expected to change quantitatively with G. However, the evaluation of this dependence is beyond the scope of the present investigation.

3.3.1. *Anisotropic heterogeneity*

In order to find out the degree to which the above observations are affected by anisotropy, we carried out a series of simulations for $l_x = 0.2$ and $l_y = 0.05$, see figure 16. For all other parameter values equal to the reference case, i.e. $Pe = 500$, $G = 1$, $R = 2$, $A = 0.5$, and $s = 0.5$, the concentration contours at different times are shown in figure 17. About the same number of fingers as in the reference case is seen to develop, but they are somewhat narrower and longer. This reflects the 'aspect ratio' of the heterogeneity distribution, which enhances the fluid flow in the streamwise direction, while inhibiting transport in the transverse direction, thereby leading to earlier breakthrough. The ability of heterogeneity anisotropy to favour one transport direction at the expense of another should affect the relative balance between the tendencies towards channelling (which involves mostly streamwise transport) and towards forming a gravity tongue (this requires a certain amount of transverse transport). As a result, the value of s_{max} resulting in maximum recovery is expected to change as a function of the degree of anisotropy. However, as was seen above, changing the length scales in order to generate this anisotropy affects the overall nature of the displacement process in several different ways, e.g. depending on whether the parameter values are close to resonant conditions or not. As a result, the influence of anisotropy on s_{max} is expected to be a function of the other parameters as well.

4. Conclusions

In the light of earlier findings for neutrally buoyant flows (Tan & Homsy 1992; Chen & Meiburg 1998*b*), permeability heterogeneities lead to some very different

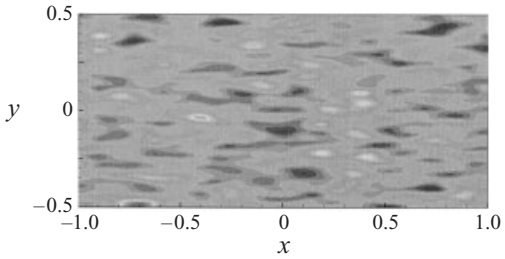

FIGURE 16. Anisotropic permeability field for $l_x = 0.2$ and $l_y = 0.05$.

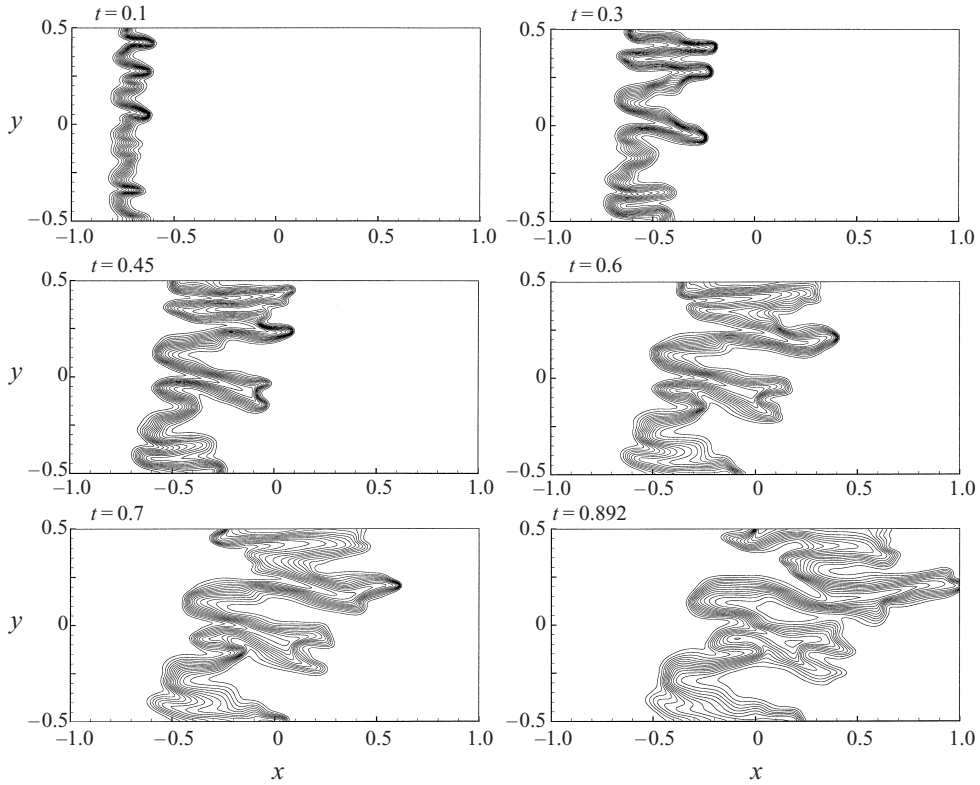

FIGURE 17. Concentration contours for $Pe = 500$, $G = 1$, $R = 2$, $A = 0.5$, and $s = 0.5$, as well as the anisotropic correlation lengths of $l_x = 0.2$ and $l_y = 0.05$. Slightly longer and narrower fingers than in the reference case are seen to develop, as the anisotropy enhances (inhibits) transport in the streamwise (transverse) direction.

effects in rectilinear displacements with density variations. The main reason for some of these unexpected findings lies in the way the heterogeneities interact with the gravity tongue observed in homogeneous flows (part 1). This gravity tongue was seen to be the result of a 'focusing' mechanism generated by the combined effects of the unfavourable viscosity gradient and the potential velocity field generated by the horizontal boundaries. The present simulations show that the vorticity associated with permeability heterogeneities systematically counteracts the effects of gravity vorticity by contributing circulation of the opposite sign. In addition, the somewhat randomly arranged vorticity dipoles associated with the heterogeneities result in a

certain amount of 'defocusing', which tends to prevent the formation of the gravity tongue. Keeping in mind earlier findings for neutrally buoyant displacements (Tan & Homsy 1992; Chen & Meiburg 1998*b*), the level of heterogeneity affects the breakthrough recovery of flows with density contrasts in a very different fashion. While for moderate heterogeneities the gravity tongue leads an to early breakthrough, the same result is accomplished for large heterogeneities by the channelling mechanism. At intermediate values of s, these mechanisms weaken each other, and the breakthrough recovery attains a maximum. This is in contrast to neutrally buoyant flows, where the breakthrough recovery usually is seen to decline monotonically with increasing levels of heterogeneity. In a similar fashion, the role of the correlation length in determining the breakthrough efficiency in a displacement with a density contrast is diametrically opposed to that in neutrally buoyant flows. For these, the recovery is typically seen to be minimal at intermediate correlation lengths, due to the resonant interaction between viscosity and permeability vorticities. For variable-density displacements, on the other hand, a gravity tongue tends to form for both very small and very large values of this length, so that the recovery reaches a maximum at intermediate values. The very different roles played by the correlation length and variance, depending on whether the displacement is neutrally buoyant or not, indicate that interesting vorticity dynamics is to be expected in three-dimensional displacements. Within horizontal planes, the roles of l and s may be more similar to neutrally buoyant flows, whereas in vertical planes, density effects might dominate.

Both the correlation length as well as the variance of the heterogeneity field were seen to affect the nature of the displacements in several different ways, depending on the values of the remaining dimensionless parameters, due to their separate influences on the individual, mutually interacting mechanisms. As a result, their overall effects on such global quantities as the breakthrough recovery cannot be parameterized easily. In addition, there are substantial differences between individual random realizations of heterogeneity fields characterized by identical correlation lengths and variances. This is particularly true for large values of s, with the reason being that for the present simulations the domain length is a relatively small multiple of the correlation length. Consequently, it would be of interest to extend the present investigation either by considering much smaller correlation lengths, or by averaging over many random realizations with identical variances and correlation lengths.

The authors would like to acknowledge several helpful discussions with Dr Hamdi Tchelepi. We also thank Dr C.-Y. Chen for providing us with the permeability field. This research is supported by the donors of The Petroleum Research Fund, administered by the American Chemical Society (Grant ACS-PRF No. 33497-AC9), and by the Chevron Petroleum Technology Company. The simulations were partially carried out at the San Diego Supercomputer Center, which is funded by the National Science Foundation.

REFERENCES

Araktingi, U. G. & Orr, F. M. 1993 Viscous fingering in heterogeneous porous media. *SPE Advanced Technology Series* **1** (1), 71–80.

Chen, C.-Y. & Meiburg, E. 1998*a* Miscible porous media displacements in the quarter five-spot configuration. Part 1. The homogeneous case. *J. Fluid Mech.* **371**, 233–268.

Chen, C.-Y. & Meiburg, E. 1998*b* Miscible porous media displacements in the quarter five-spot configuration. Part 2. Effect of heterogeneities. *J. Fluid Mech.* **371**, 269–299.

Dagan, G. 1987 Theory of solute transport by groundwater. *Ann. Rev. Fluid Mech.* **19**, 183–215.

De Wit, A. & Homsy, G. M. 1997*a* Viscous fingering in periodically heterogeneous porous media. I. Formulation and linear instability. *J. Chem. Phys.* **107**, 9609–9618.

De Wit, A. & Homsy, G. M. 1997*b* Viscous fingering in periodically heterogeneous porous media. I. Numerical simulations. *J. Chem. Phys.* **107**, 9619–9628.

Gottlieb, D. & Orszag, S. A. 1977 *Numerical Analysis of Spectral Methods: Theory and Applications.* SIAM.

Koch, D. L. & Brady, J. F. 1988 Anomalous diffusion in heterogeneous porous media. *Phys. Fluids* **31**, 965.

Lele S. K. 1992 Compact finite difference schemes with spectral-like resolution. *J. Comput. Phys.* **103**, 16–42.

Moisses, D. E., Miller, C. A. & Wheeler, M. F. 1989 Simulation of miscible viscous fingering using a modified method of characteristics: effects of gravity and heterogeneity. *SPE Paper* 18440, presented at the 1989 Tenth Symposium on Reservoir Simulation, Houston, TX, February.

Ruith, M. & Meiburg, E. 2000 Miscible rectilinear displacements with gravity override. Part 1. Homogeneous porous medium. *J. Fluid Mech.* **420**, 225–257.

Shinozuka, M. & Jen, C.-M. 1972 Digital simulation of random processes and its applications. *J. Sound Vib.* **25**, 111.

Sorbie, K. S., Feghi, F., Pickup, G. E., Ringrose, P. S. & Jensen, J. L. 1992 Flow regimes in miscible displacement in heterogeneous correlated random fields. *SPE Paper* 24140, presented at the 1992 SPE/DOE Eighth Symposium on Enhanced Oil Recovery. Tulsa, OK, April.

Tan, C. T. & Homsy, G. M. 1992 Viscous fingering with permeability heterogeneity. *Phys. Fluids* A **4**, 1099–1101.

Tchelepi, H. A. 1994 Viscous fingering, gravity segregation and permeability heterogeneity in two-dimensional and three-dimensional flows. Dissertation, Department of Petroleum Engineering, School of Earth Sciences, Stanford University.

Waggoner, J. R., Casillo, J. L. & Lake, L. W. 1992 Simulation of EOR Processes in Stochastically Generated Permeable Media. *SPE Formation Eval.*, 173–180.

Wray, A. A. 1991 Minimal storage time-advancement schemes for spectral methods. Preprint.